

Defect-Site Promoted Surface Reorganization in Nanocrystalline Ceria for the Low-Temperature Activation of Ethylbenzene

B. Murugan and A. V. Ramaswamy*

Department of Chemistry, University of Pune, Pune 411007, India

Received September 21, 2006; E-mail: avram@chem.unipune.ernet.in

The study of the defective surface sites of many oxides has received considerable interest, as these sites are coordinately unsaturated and exhibit extraordinary activity in many catalytic reactions.¹ Most of the research work in this particular area is mainly focused on theoretical simulations.² However, the influence of the defect sites on the chemical nature of the oxide surface and their role in the mechanism of activation of a substrate have not yet been fully explored. In this Communication, we take the example of ceria and provide direct evidence wherein the defect-site-enriched oxide promotes the surface reorganization and thereby influences the activation of ethylbenzene (EB) in the oxidative dehydrogenation in presence of N₂O.

Ceria is an interesting oxide and is one of the constituents in many catalyst formulations.³ The method of preparation strongly influences the structural and surface properties of ceria.⁴ We intend to explore its catalytic activity in the oxidative dehydrogenation (ODH) of ethylbenzene using N₂O. A nanocrystalline ceria sample enriched with Ce³⁺–O[–]–Ce⁴⁺-type defect sites was prepared by the alcoholysis method (ceria-A). For comparison, three other ceria samples were prepared, one by conventional precipitation and the other two by a solution-combustion method using urea and glycine as fuels (ceria-P, -U and -G), respectively, as reported elsewhere.⁴

Interestingly, the nanocrystalline ceria prepared by the alcoholysis method exhibits Ce³⁺–O[–]–Ce⁴⁺-type defect sites predominantly confined to the surface, as evidenced from diffuse reflectance UV–visible spectroscopy (a weak band at around 650 nm).⁵ A rough estimate of the surface to bulk defect ratio follows the order Ceria-A > Ceria-G > Ceria-U/P based on the EPR spectroscopic analysis⁶ (Supporting Information, Figure S1) and the temperature programmed reduction⁷ of the samples (Figure S2). These defect sites promote the dehydrogenation of EB using N₂O at 598 K, which is far lower than the temperatures normally encountered in the existing conventional processes for the dehydrogenation of EB (873 K). An equilibrium conversion of 45 mol % and a styrene selectivity of 94%, comparable to that obtained in commercial practice are achieved by the ceria catalyst prepared by the alcoholysis method. However, the ceria samples prepared by conventional and combustion methods showed comparable activity and selectivity to styrene at much higher activation temperatures (Ceria-G at 648 K and Ceria-U/P at 723 K).

To address the role of defect sites in governing the temperature of activation, EPR investigations were done on the ceria samples by subjecting each one of them to hydrogen treatment, as the dehydrogenation process involves interaction of hydrogen atoms with the catalyst surface. Figure 1 shows the direct correlation between the concentrations of Ce³⁺–O[–]–Ce⁴⁺-type defect sites [at $g_{\perp} = 1.96$ and $g_{\parallel} = 1.933$ (D signal) and 1.940 (A signal)] and the temperature of activation. In the case of defect-site-enriched ceria-A sample, the concentration of defect sites remained almost unaffected upon treatment with hydrogen up to a temperature of about 573 K. A steep decrease in the concentration of Ce³⁺–O[–]–Ce⁴⁺-type

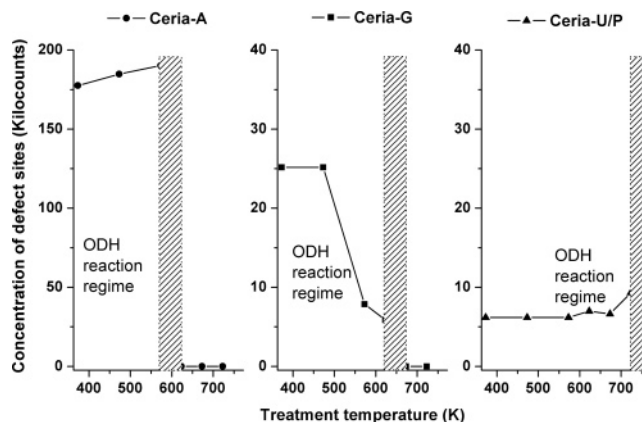


Figure 1. The concentration of defect sites (Ce³⁺–O[–]–Ce⁴⁺) as determined from the EPR signal intensity ($g_{\perp} = 1.96$) as a function of hydrogen treatment temperature.

defect site to almost zero occurs when the temperature of hydrogen treatment is increased to 623 K.

This sudden disappearance of the signal because of the defect site is attributed to the surface reorganization of ceria.⁵ In nanocrystalline ceria the variation in the signal intensities upon increase in the reduction temperature indicates the migration of subsurface oxygen. The migrated oxygen from the subsurface reoxidizes the Ce³⁺ ions and thus causes a sudden disappearance of the signal owing to the defect Ce³⁺ ions. This subsurface oxygen migration occurs at a lower temperature in the case of ceria sample prepared by the alcoholysis method (573–623 K), whereas it occurs relatively at higher temperatures in the case of ceria samples prepared by the glycine combustion method (623–673 K) and urea combustion/precipitation methods (723–773 K). This indicates that the presence of a Ce³⁺–O[–]–Ce⁴⁺-type defect site promotes the oxygen ion mobility and thus supports the surface reorganization. The oxygen ion mobility from the subsurface at the ODH temperature regime is confirmed further by the increase in signal intensity of electron deficient surface oxygen anion O_s[–] species ($g_{\perp} = 2.035$ and $g_{\parallel} = 2.001$) in EPR analysis.^{1b}

The above EPR studies clearly indicate that the oxygen migration from the subsurface is directly related to the concentration of defective sites and further relates to the temperature of activation. A correlation between the concentration of defect sites of different ceria samples prepared by different methods and the temperature required for 50 mol % conversion of EB T_{50} (a normal activity parameter for many exothermic reactions) is given in Figure 2. The equilibrium conversion and selectivity can be achieved in various ceria samples at their respective temperature regime. The observed decrease in the EPR signal intensity corresponding to Ce³⁺–O[–]–Ce⁴⁺-type defect sites by the in situ adsorption of ethylbenzene at different temperatures on ceria samples (Figure 3a)

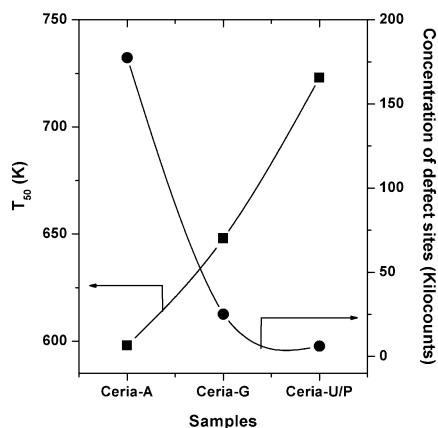


Figure 2. Dependence of the concentration of defect sites and the activation temperature required for 50 mol % conversion of ethylbenzene (T_{50}) for the different ceria samples prepared by different routes.

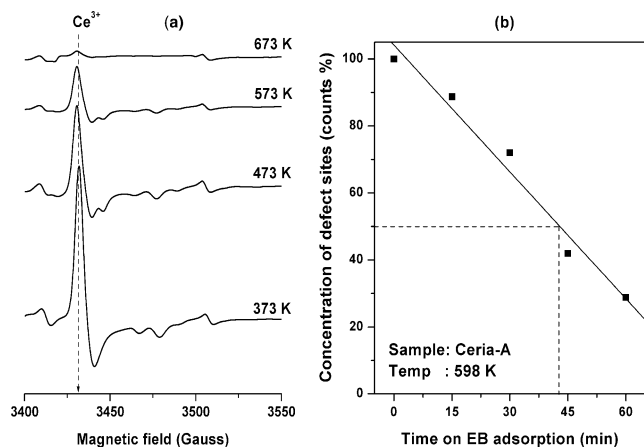


Figure 3. (a) Representative EPR spectra of a ceria sample prepared by alcoholysis method (Cerria-A) after in situ adsorption of ethylbenzene at various temperatures and recorded at 298 K. Adsorption of ethylbenzene vapors was carried out for a period of 1 h with an EB flow rate of 2.3 mL h^{-1} at respective temperatures. (b) Variation in the concentration of defect sites, as recorded from the EPR signal intensity, with time on adsorption of EB on a ceria sample prepared by alcoholysis method (Cerria-A) at 598 K.

further indicates that these sites are responsible for the activation of α and β -hydrogen of ethylbenzene substrate.

To understand whether the concentration of Ce^{3+} defect sites can limit the rate of the reaction, a time on stream study was conducted by in situ adsorption of ethylbenzene at 598 K on a ceria sample prepared by the alcoholysis method (Figure 3b). Interestingly, the rate of decrease in the EPR signal intensity, a measure of Ce^{3+} defect sites, was about 1.26 count % per min which was found to be in the same order of magnitude with that of the rate of EB conversion (1.11 mol % per min). The time required for the Cerria-A sample to achieve 50% conversion of EB at 598 K is approximately 45 min, which is comparable to the time required for the 50% decrease in the defect site concentration (Figure 3b). Thus, we can suggest that the presence of a $\text{Ce}^{3+}-\text{O}^{-}-\text{Ce}^{4+}$ -type defect site is kinetically significant in determining the rate of ODH of EB.

In most of the oxidation reactions involving metal oxides as catalysts, the rate-determining step is the surface reaction that

involves the lattice oxygen (O^{2-} or O^{-} as a part of the lattice defect site). Once the lattice oxygen is transferred to the substrate, there are two processes that occur: (a) the migration of sub-lattice oxygen to the surface and (b) the replenishment of the oxygen ion vacancy from the gas phase to the bulk. These latter two steps are known to be faster than the catalytic step (dissociation of α and β -hydrogen of ethylbenzene).⁸ In the present study, the ODH turnover rates increased as the concentration of surface-defect sites increased, suggesting that the activation of α and β -hydrogen of ethylbenzene substrate by the $\text{Ce}^{3+}-\text{O}^{-}-\text{Ce}^{4+}$ -type surface-defect sites is the rate-determining step.⁹ Hence, under steady-state conditions, the rate of vacancy migration or oxygen ion mobility from the bulk to the surface will not be limiting on the catalytic rate.

From the above investigations, we can propose a catalytic pathway for the oxidative dehydrogenation of ethylbenzene on ceria using N_2O as the oxidant, considering that this ODH reaction follows a Mars-van Krevelen mechanism (Scheme S1). We can conclude that a ceria sample enriched with surface $\text{Ce}^{3+}-\text{O}^{-}-\text{Ce}^{4+}$ -type defect sites promotes the subsurface oxygen migration and thus facilitates surface reorganization. This favors a lower temperature of activation of the substrate. We find a direct relationship between the concentration of the defect sites and the energy required for the activation of the substrate on the one hand and a correlation between the rate of EB conversion and the rate of consumption of the defect sites on the other.

Acknowledgment. We are grateful to Dr. D. Srinivas, Dr. C. V. Satyanarayana, and Dr. Veda Ramaswamy of National Chemical Laboratory, Pune, for their contributions to the experimental data and fruitful discussions. We thank CSIR, New Delhi, for the financial support (Grant ES 21(0561)/03/EMR-II).

Supporting Information Available: Experimental part, Figures S1 and S2, and Scheme S1. This material is available free of charge via the Internet at <http://pubs.acs.org>.

References

- (1) (a) Yan, Z.; Chinta, S.; Mohamed, A. A.; Fackler, J. P., Jr.; Goodman, D. W. *J. Am. Chem. Soc.* **2005**, *127*, 1604–1605. (b) Sterrer, M.; Diwald, O.; Knozinger, E. *J. Phys. Chem. B* **2000**, *104*, 3601–3607.
- (2) (a) Sanchez, A.; Abbet, S.; Heiz, U.; Schneider, W.-D.; Halkkinen, H.; Barnett, R. N.; Landman, U. *J. Phys. Chem. A* **1999**, *103*, 9573–9578. (b) Costuas, K.; Parrinello, M. *J. Phys. Chem. B* **2002**, *106*, 4477–4481. (c) Orlando, R.; Millini, R.; Perego, G.; Dovesi, R. *J. Mol. Catal. A* **1997**, *119*, 253–262. (d) Kolmel, C.; Ewig, C. S. *J. Phys. Chem. B* **2001**, *105*, 8538–8543. (e) Ferrari, A. M.; Giordano, L.; Rosch, N.; Heiz, U.; Abbet, S.; Sanchez, A.; Pacchioni, G. *J. Phys. Chem. B* **2000**, *104*, 10612–10617. (f) Valentin, C. D.; Pacchioni, G.; Abbet, S.; Heiz, U. *J. Phys. Chem. B* **2002**, *106*, 7666–7673.
- (3) (a) Trovarelli, A.; Leitenburg, C. d.; Boaro, M.; Dolcetti, G. *Catal. Today* **1999**, *50*, 353–367. (b) O'Hara, F. J. U.S. Patent 3 904 552, 1975. (c) Sherrod, F. A.; Smith, A. R. U.S. Patent 4 758 543, 1988. (d) Murakamy, A.; Unei, H.; Teranishi, M.; Ohta, M. U.S. Patent 5 190 906, 1993.
- (4) Murugan, B.; Ramaswamy, A. V.; Srinivas, D.; Gopinath, C. S.; Ramaswamy, V. *Chem. Mater.* **2005**, *17*, 3983–3993.
- (5) Binet, C.; Badri, A.; Lavalley, J. C. *J. Phys. Chem.* **1994**, *98*, 6392–6398.
- (6) (a) Abi-Aad, E.; Bechara, R.; Grimblot, J.; Aboukais, A. *Chem. Mater.* **1993**, *5*, 793–797. (b) Abi-Aad, E.; Bennani, A.; Bonnelle, J.-P. *J. Chem. Soc., Faraday Trans.* **1995**, *91*, 99–104.
- (7) Damyanova, S.; Perez, C. A.; Schmal, M.; Bueno, J. M. C. *Appl. Catal. A* **2002**, *234*, 271.
- (8) Shin, M. Y.; Chung, K. S.; Hwang, D. W.; Chung, J. S.; Kim, Y. G.; Lee, J. S. *Langmuir* **2000**, *16*, 1109–1113.
- (9) Chen, K.; Bell, A. T.; Iglesia, E. *J. Catal.* **2002**, *209*, 35–42.

JA066834K